



The dynamics of cylindrical samples in dual wind-up extensional rheometers

Yu, Kaijia; Rasmussen, Henrik K.; Marín, Jose Manuel Román; Hassager, Ole

Published in:
Journal of Rheology

Link to article, DOI:
[10.1122/1.3568816](https://doi.org/10.1122/1.3568816)

Publication date:
2011

[Link back to DTU Orbit](#)

Citation (APA):

Yu, K., Rasmussen, H. K., Marín, J. M. R., & Hassager, O. (2011). The dynamics of cylindrical samples in dual wind-up extensional rheometers. *Journal of Rheology*, 55(3), 571-580. <https://doi.org/10.1122/1.3568816>

General rights

Copyright and moral rights for the publications made accessible in the public portal are retained by the authors and/or other copyright owners and it is a condition of accessing publications that users recognise and abide by the legal requirements associated with these rights.

- Users may download and print one copy of any publication from the public portal for the purpose of private study or research.
- You may not further distribute the material or use it for any profit-making activity or commercial gain
- You may freely distribute the URL identifying the publication in the public portal

If you believe that this document breaches copyright please contact us providing details, and we will remove access to the work immediately and investigate your claim.

The dynamics of cylindrical samples in dual wind-up extensional rheometers

Kaijia Yu and Henrik Koblitz Rasmussen^{a)}

*Department of Mechanical Engineering, Technical University of Denmark,
DK-2800 Kgs. Lyngby, Denmark*

Jose Manuel Román Marín and Ole Hassager

*Department of Chemical and Biochemical Engineering, Technical University
of Denmark, DK-2800 Kgs. Lyngby, Denmark*

(Received 12 May 2010; final revision received 10 February 2011;
published 22 March 2011)

Synopsis

Numerical computations of the extension of circular cylindrical shaped samples in a dual wind-up drum rheometer of Sentmanat extensional rheometer type [M. L. Sentmanat, *Rheol. Acta* **43**, 657 (2004); R. Garritano and H. Berting, US Patent No. 7,096,728 (08/29/2006)] are presented. These time-dependent computations are fully three dimensional and based on theoretically ideal configurations. If necking or sample rupture does not occur, the elongation will resemble as ideal uni-axial if the initial sample diameter is decreased sufficiently. An initial diameter larger than 0.5 mm may result in large deviations from ideal uni-axial deformation. © 2011 The Society of Rheology. [DOI: 10.1122/1.3568816]

I. INTRODUCTION

The measurements of stress-strain relations in the wide variety of existing rheometers are all based on the assumption of a homogeneous deforming sample. It may be throughout the whole sample or in a local area, depending of the type of rheometer. A lot of theoretical effort has therefore been devoted to discuss this assumption, both in shear [Adams and Olmsted (2009)] as well as extension. Here, our concern is the consideration of uni-axial extension. In extension the currently used rheometers are the Münstedt tensile rheometer (MTR) [Münstedt (1979)], the Meissner elongational rheometer [Meissner and Hostettler (1994)], the filament stretch rheometer (FSR) [Sridhar *et al.* (1991)], and the recent Sentmanat extensional rheometer (SER) [Sentmanat (2004)]. These rheometers are commonly used to characterize entangled polymeric liquids and elastomers, as extensional flow measurements are very sensitive to the molecular structure. In particular the FSR has received [Kolte *et al.* (1997); Sizaïre and Legat (1997); Rasmussen and Hassager (2001)] and still does receive [Webster *et al.* (2008)] a lot of theoretical attention. Although the FSR and MTR are technically very different, they theoretically fall within the same frame. They both consider a cylindrical polymer sample held between two

^{a)}Electronic mail: hkra@mek.dtu.dk

plates that are pulled apart to induce the extensional flow. The SER fixture consists of two cylindrical drums where a strip is attached. The sample is extended by rotating both drums in opposite directions. For dual wind-up methods as the SER and RME only the very recent SER computational studies by Yu *et al.* (2010) and Hassager *et al.* (2010) exist.

The original work by Sentmanat (2004) as well as the studies by Yu *et al.* (2010) and Hassager *et al.* (2010) considers the extension of rectangular shaped strips, whereas experimental studies, on the SER, with monodisperse [Wang and Wang (2008)] and bidisperse [Auhl *et al.* (2009)] polymer melts have according to our knowledge mainly been performed applying (circular) cylindrical samples. Measurements on these types of materials lay the foundation for the understanding of the physics of polymeric systems [Marrucci and Ianniruberto (2004); Schieber *et al.* (2007); Wagner *et al.* (2008); Nielsen and Rasmussen (2008); Nielsen *et al.* (2008); Dhole *et al.* (2009); Rasmussen *et al.* (2009)]. Therefore, it is particularly important to know what extent these measurements represent ideal uniaxial deformation. Experimental studies of the SER technique applying a cylindrical sample, with regard to the uniformity of the extensional deformation, have according to our knowledge not been published yet. The influence of the material as well as the initial geometry of the sample is currently unclear. Here, the purpose is to discuss the potential deviations from ideal uni-axial deformation using (circular) cylindrical samples on a SER, based solely on numerical computations of theoretically ideal configurations.

II. EXTENSION OF CYLINDRICAL SAMPLES IN THE SER

The SER consists of two cylindrical drums as illustrated in Fig. 1(a). A sample here shaped as a circular cylinder with an initial diameter D_0 is attached onto these drums. The extension is achieved by rotating the drums in opposite directions with the same constant rotation rate Ω . The set extension rate applied to the sample or commonly referred to as the nominal Hencky strain rate is then expressed as

$$\dot{\epsilon}_N = \frac{2\Omega R}{L_0}. \quad (1)$$

R is the radius of the equally dimensioned wind-up drums and L_0 is the centerline distance between the two drums. As illustrated in Fig. 1(a), L_0 is also equal to the initial length of the unsupported part of the sample. Notice from a theoretical perspective that the SER and the extensional viscosity fixture (EVF) rheometer [Garritano and Berting (2006)] are identical techniques.

In all our simulations the initial shape of the tested specimen is a cylinder with an unsupported length (L_0) of 12.7 mm and a diameter (D_0) of 0.5, 1, or 2 mm, as the maximal reported initial sample diameter is 2 mm [Wang *et al.* (2007); Wang and Wang (2008)]. The radius of the wind-up drums R is 5.1 mm. The nominal Hencky strain itself is

$$\epsilon_N = \dot{\epsilon}_N t, \quad (2)$$

where t is the time from the start of the extension. At time $t=0$ the rolls start the rotation with a constant angular velocity. Experimentally, as well as computationally, the sample is assumed to be stress free and at rest initially. In this work the third order accurate, in time and space, Lagrangian finite element method developed by Marín and Rasmussen (2009) is used in the computations. The variables are the spatial coordinates attached to the particles. These Lagrangian variables enable the method to handle arbitrary large

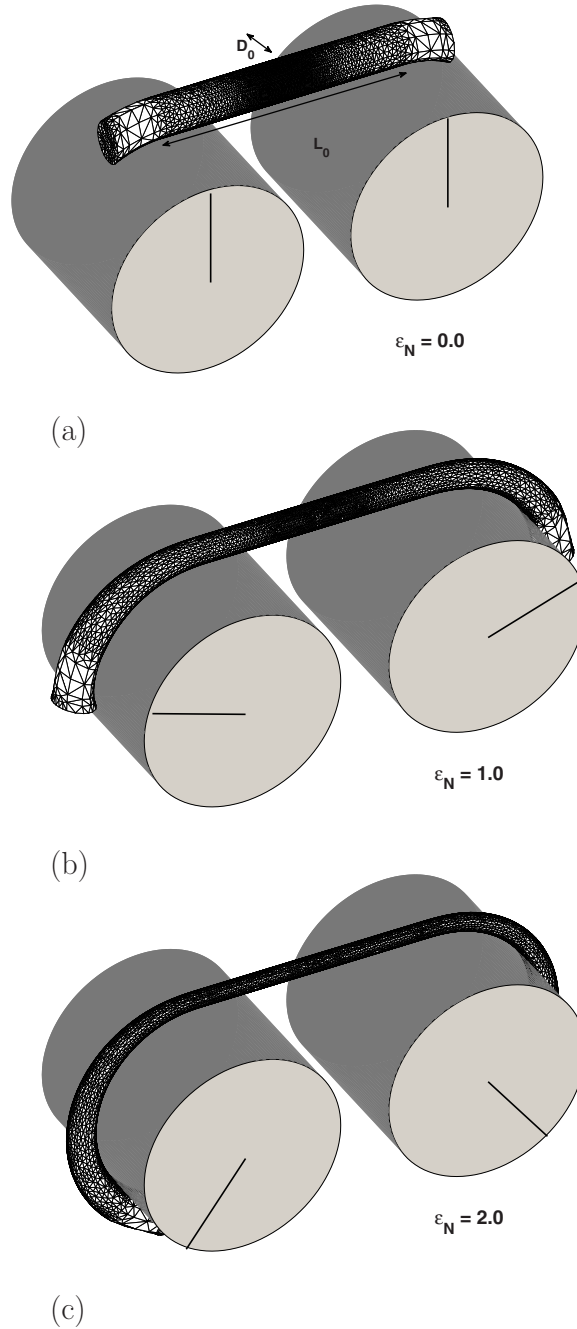


FIG. 1. Simulation of a circular cylindrical sample in the SER. D_0 is the initial diameter of the sample and L_0 is the distance between the rotational axes of the drums. The diameter is $D_0 = 2$ mm.

movement of particles in surfaces and interfaces, as well as an easy handling of dynamic contact lines [Rasmussen *et al.* (2000)]. In our computations the node points contacting with the drums are prescribed non-slip boundary conditions, and they are advected according to the motion of the rolls [Yu *et al.* (2010)] as illustrated in Figs. 1(b) and 1(c).

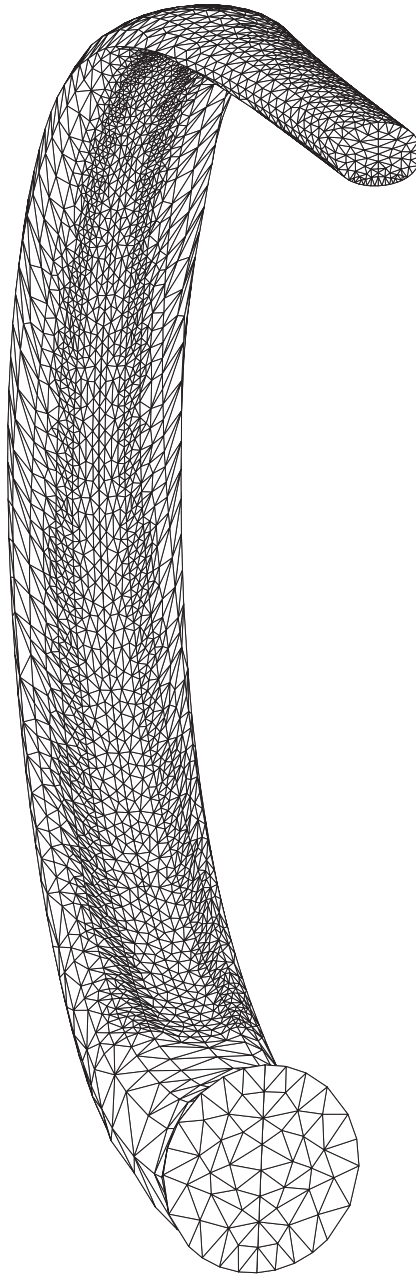


FIG. 2. Simulation of the extension of a neo-Hookean sample in the SER. The initial sample diameter is $D_0 = 2$ mm. The finite element mesh corresponds to half of the sample. The nominal Hencky strain is $\epsilon_N = 2.3$.

The extension in any stretching apparatus is not uniform throughout the sample as the sample sticks to the end fixtures. Nevertheless, the assumption of a homogeneous deformation in the center of the sample should be sufficient to obtain a correct extensional measurement [Szabo (1997)]. For the SER this is illustrated in Fig. 2 where a $D_0 = 2$ mm sample described by the neo-Hookean elastic model is extended. Near the rolls the sample does not resemble a circular cylinder. The contact to the rollers combined with

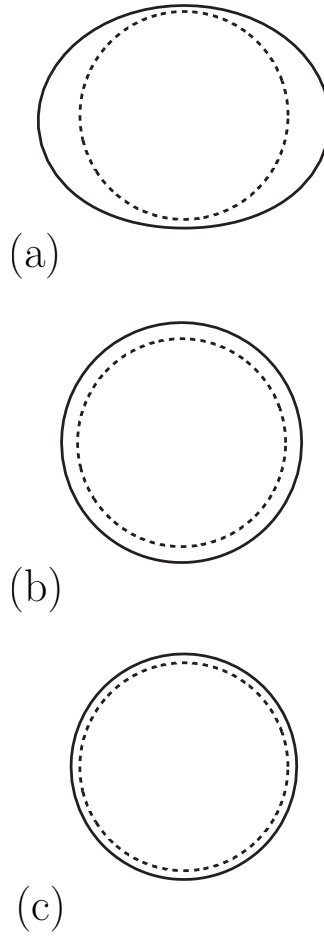


FIG. 3. Surface contours at the mid-plane of the sample at $\epsilon_N=2.3$. The simulation (solid lines) is based on (a) the neo-Hookean model and the MSF model (6) at (b) $De=10\,000$ and (c) $De=1$. The dashed lines are the expected contour assuming ideal uni-axial deformation. The initial sample diameter is $D_0=2$ mm.

the extensional force has flattened the sample. This affects even the central part of it. Figure 3(a) shows the surface contour at the mid-plane of the neo-Hookean sample as the solid line at a nominal Hencky strain of 2.3. The dashed circles are the surface contour assuming ideal uni-axial deformation. The deformation neither has the correct strain nor follows uni-axial which is reflected in a circular surface contour.

In Fig. 4 we present a more exhaustive analysis of the influence of the initial sample radius. As it is customary in the experimental validation of the strain rate in the SER technique, we show the evolution of a specimen's diameter $[D(t)]$ in the direction of the rotational axis of the drums. As seen in Figs. 2 and 3(a), this is the direction that exhibits the largest deviation from the ideal case. We calculate it as a Hencky strain based on this sample diameter, defined as

$$\epsilon_D = 2 \ln \left(\frac{D_0}{D(t)} \right). \quad (3)$$

Ideally, the diameter of a circular cross-section polymeric sample should follow the expression $\epsilon_D = \epsilon_N$. If this requirement fails the deformation is not a constant strain rate

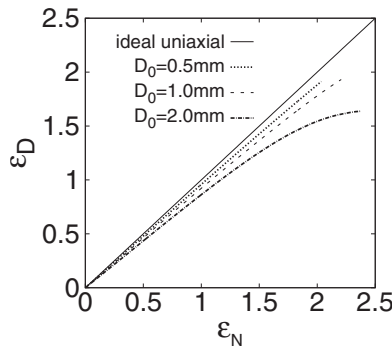


FIG. 4. Simulations of the extension of neo-Hookean elastomer. The Hencky strain based on sample diameter ϵ_D [see Eq. (3)] is shown as a function of the nominal Hencky strain ϵ_N [see Eq. (2)], and the solid line represents ideal uni-axial deformation ($\epsilon_D = \epsilon_N$). The simulations show the influence of the initial diameter: $D_0 = 0.5, 1$, and 2 mm.

uni-axial deformation. The different simulations in Fig. 4 are performed varying the initial diameter of the polymer samples. Although the neo-Hookean model exhibits a severe deviation from ideal uni-axial elongation at large initial values of the diameter, this deviation gradually disappears as the initial diameter is reduced. We have not reported the geometrical values non-dimensionally, but due to the geometrical restrictions on the SER fixture one non-dimensional sample diameter may be applied.

In the work by Yu *et al.* (2010) and Hassager *et al.* (2010), discussing the extension of rectangular shaped strips in the SER, the importance of the weighting between the Cauchy and Finger strain tensors in the constitutive equation was particularly emphasized, as well as the amount of elasticity in the sample. The components of stress tensor (σ_{ij}) of the neo-Hookean elastic model only depend on the Finger strain tensor as $\sigma_{ij} = 3G \langle E_{in} u_n E_{jm} u_m \rangle$, where G is the shear modulus. Notice that the components of the deformation gradient tensor, \mathbf{E} , are given as $E_{ij}(\mathbf{x}, t, t') = \partial x_i / \partial x'_j$, with $i = 1, 2, 3$ and $j = 1, 2, 3$, where the coordinates of a given particle, (x'_1, x'_2, x'_3) , in the stress free reference state (at time t') are displaced to coordinates (x_1, x_2, x_3) in the current state (at time t). The angular brackets denote an average over a unit sphere $\langle \dots \rangle = 1 / (4\pi) \int_{|\mathbf{u}|=1} \dots d\mathbf{u}$, where \mathbf{u} is a unit vector.

For polymer melts and entangled liquids there exists a large amount of experiments suggesting that the dynamics should be based on the independent alignment tensor from the Doi–Edwards reptation theory [Doi and Edwards (1978)]. As a consequence the deviations from ideal uni-axial extension are different in the extension of elastomers and melts in the SER. Here, we will focus particularly on the dynamics of monodisperse polymer melts. As suggested by Wagner *et al.* (2005) we will add a stretch equation based on the “interchain pressure” concept [Marrucci and Ianniruberto (2004)] on the constitutive model by Doi and Edwards (1978). This approach seems to be capable of predicting the flow behavior of linear as well as branched monodisperse polymer melts [Nielsen and Rasmussen (2008); Wagner and Rolón-Garrido (2010); Rasmussen *et al.* (2009)]. The constitutive model without a maximal extensibility of the polymer is

$$\sigma_{ij} = \int_{-\infty}^t M(t-t') f(t, t')^2 5 \left\langle \frac{E_{in} u_n E_{jm} u_m}{|\mathbf{E} \cdot \mathbf{u}|^2} \right\rangle dt', \quad (4)$$

where

$$\frac{\partial}{\partial t}f(t, t') = f(t, t') \left[\frac{\partial}{\partial t} \langle \ln |\mathbf{E} \cdot \mathbf{u}| \rangle - \frac{1}{\tau_w} f(t, t') (f(t, t')^3 - 1) \right], \quad f(t', t') = 1, \quad (5)$$

where τ_w is the relaxation time of the tube diameter. The linear dynamics of the polymer is described by the memory function $M(t-t')$ and f is referred to as the molecular stress function (MSF). For simplicity we will only use an approximation of the MSF. The applied f is the (analytical) solution of the differential equation

$$\begin{aligned} \frac{\partial}{\partial t}f(t, t') &= -\frac{1}{\tau_w} f(t, t')^2 (f(t, t')^3 - 1) \quad \text{with the initial condition} \\ f(t', t') &= \exp(\langle \ln |\mathbf{E} \cdot \mathbf{u}| \rangle). \end{aligned} \quad (6)$$

This corresponds to the exact solution in the case of ideal stress relaxation. The constitutive equation is then a KBKZ (Kaye, Bernstein, Kearsley, and Zapas) approximation of the “interchain pressure” version of the MSF constitutive model [Wagner and Schaeffer (1992)]. A similar approach, although using a simplified MSF of Rouse type, has been used before [Lyhne *et al.* (2009)] to model and predict the delayed rupture of extended monodisperse polymer melts during stress relaxation. In our computations we apply the Currie approximation [Currie (1982)] for the terms in the angular brackets in the Eqs. (4)–(6).

For the memory function we apply the method by Baumgaertel, Schausberger, and Winter (BSW) [Baumgaertel *et al.* (1990)]. The relaxation spectrum of the BSW model representing a continuous distribution of time constant is

$$G(t-t') = \int_0^\infty \frac{H(\tau)}{\tau} e^{-(t-t')/\tau} d\tau, \quad (7)$$

$$H(\tau) = n_e G_N^0 \left[\left(\frac{\tau}{\tau_{\max}} \right)^{n_e} + \left(\frac{\tau}{\tau_c} \right)^{-n_g} \right] h(1 - \tau/\tau_{\max}), \quad (8)$$

where $h(x)$ is the Heaviside step function and τ_{\max} is the maximal relaxation time constant in the dynamics of the polymer. The plateau modulus (G_N^0), τ_c , n_e , and n_g are material parameters with unique values for each type of polymer. The relation between the memory function and relaxation modulus is $M(t-t') = dG(t-t')/dt'$.

Here, we apply a Deborah number based on the largest linear relaxation time as $De = \dot{\epsilon}_N \tau_{\max}$ and use the material parameters obtained for a 390 kg/mol monodisperse polystyrene in our computations. All material parameters in the BSW model can be found in Bach *et al.* (2003), and we do have the ratio $\tau_{\max}/(\tau_w/3) = 28.7$ from Wagner *et al.* (2005).

The unstructured mesh used in all the presented simulations contains 17 358 elements with emphasis on refining the mesh where the elements are mostly needed, and it is shown in detail in Fig. 2. For cases with a dynamic contact surface, an unstructured mesh is preferred as it ensures a gradual attachment of nodal coordinates onto the rollers. The mesh is particularly refined at the contact area against the rollers. To ensure that the computations are sufficiently accurate, we have performed neo-Hookean computations with two crude meshes as well, one with 318 elements and another with 1369 elements using an initial sample diameter of $D_0 = 2$ mm. At a nominal Hencky strain of 1.5 the fine mesh with 17 300 elements gave a diameter $D = 0.534$ mm, the mesh with 1369 elements

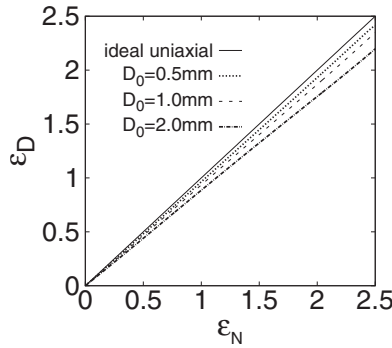


FIG. 5. Simulations of the extension of a melt based on the MSF model in Eq. (6) at a Deborah number of $De=10\,000$. The Hencky strain based on sample diameter ϵ_D [see Eq. (3)] is shown as a function of the nominal Hencky strain ϵ_N [see Eq. (2)], and the solid line represents ideal uni-axial deformation ($\epsilon_D=\epsilon_N$). The simulations show the influence of the initial diameter: $D_0=0.5$, 1, and 2 mm.

gave a value of $D=0.531$ mm, and the very crude mesh using 318 elements gave a value of $D/D_0=0.527$ mm. So the computational accuracy of the most refined mesh is expected to be a few thousandths.

Figure 3(b) shows the surface contour at the Deborah number of 10 000 at the mid-plane of the $D_0=2$ mm sample at $\epsilon_N=2.3$. A Deborah number of 10 000 represents an extension in the limit of an elastic deformation. Although the strain deviates significantly from the ideal case (dashed line), the computations (solid line) show a circular surface contour which indicates uniaxial deformation in the center.

In Fig. 5 we present computations of the influence of the initial sample radius on the diameter based Hencky strain for the above model in Eqs. (4) and (6) at a fixed Deborah number of 10 000. The neo-Hookean model (see Fig. 3) does represent the most severe deviation from the ideal case. But the above model still represents a large deviation from the ideal case. For a sample with initial diameter $D_0=2$ mm, the diameter based Hencky strain is 0.3 units below the ideal one at a nominal Hencky strain of 2.5. This deviation reduces almost linearly with the initial diameter D_0 .

In Fig. 6 we have compared the neo-Hookean with the model represented by Eqs. (4)

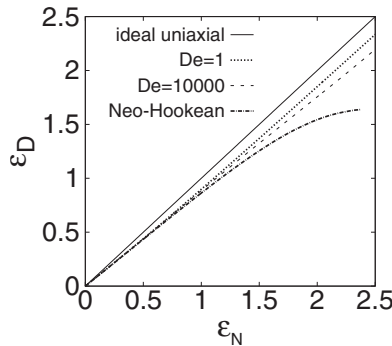


FIG. 6. Simulations of the extension of an elastomer and a polymer melt. The simulations are based on the neo-Hookean model and the MSF model in Eq. (6) at Deborah numbers of $De=10\,000$ and $De=1$. The initial diameter of the sample is fixed at $D_0=2$ mm. The Hencky strain based on sample diameter ϵ_D [see Eq. (3)] is shown as a function of the nominal Hencky strain ϵ_N [see Eq. (2)], and the solid line represents ideal uni-axial deformation ($\epsilon_D=\epsilon_N$).

and (6) at both Deborah numbers of 10 000 and 1. The latter represents a low amount of elasticity as well as a strain softening material. As already recognized in the work by Yu *et al.* (2010), this reduces the deviation from the ideal case. All our performed computations for the model in Eqs. (4) and (6) result in a circular shaped (e.g., uniaxial deformation) surface contour [shown as the solid line in Figs. 3(b) and 3(c)] in the center of the sample for all applied initial diameters as well as Deborah numbers.

One has to keep in mind that a ductile failure or necking can appear in the sample in the SER [Sentmanat *et al.* (2005); Wang *et al.* (2007)]. An appearance of a ductile necking during the measurements leads to a complete loss of symmetry as well as homogeneity and eventually to a sample breakage. The ductile failure is an important limitation not only in the use of the SER but also in the use of almost all extensional rheometers. The only exception seems to be the FSR. It has shown in several cases the ability to prevent the ductile failure [Bach *et al.* (2003); Rasmussen *et al.* (2005)].

III. CONCLUSION

The computations of the extension of a (circular) cylindrical sample in the SER show that the elongation resembles to ideal behavior when the initial sample diameter is decreased sufficiently. The use of a sample with a diameter of 1 mm may result in more than 10% deviation from the expected Hencky strain. The exact value of the deviation may be difficult to quantify as the constitutive behavior of a measured substance in most cases is likely to be unknown.

ACKNOWLEDGMENT

The authors gratefully acknowledge financial support from the “Direktr, dr. Techn. A.N. Neergaards og Hustrus Fond” Foundation.

References

- Adams, J. M., and P. D. Olmsted, “Nonmonotonic models are not necessary to obtain shear banding phenomena in entangled polymer solutions,” *Phys. Rev. Lett.* **103**, 219801 (2009).
- Auhl, D., P. Chambon, T. C. B. McLeish, and D. J. Read, “Elongational flow of blends of long and short polymers: Effective stretch relaxation time,” *Phys. Rev. Lett.* **103**, 136001 (2009).
- Bach, A., K. Almdal, H. K. Rasmussen, and O. Hassager, “Elongational viscosity of narrow molar mass distribution polystyrene,” *Macromolecules* **36**, 5174–5179 (2003).
- Baumgaertel, M., A. Schausberger, and H. H. Winter, “The relaxation of polymers with linear flexible chains of uniform length,” *Rheol. Acta* **29**, 400–408 (1990).
- Currie, P. K., “Constitutive equations for polymer melts predicted by the Doi–Edwards and Curtiss–Bird kinetic theory models,” *J. Non-Newtonian Fluid Mech.* **11**, 53–68 (1982).
- Dhole, S., A. Leygue, C. Bailly, and R. Keunings, “A single segment differential tube model with interchain tube pressure effect,” *J. Non-Newtonian Fluid Mech.* **161**, 10–18 (2009).
- Doi, M., and S. F. Edwards, “Dynamics of concentrated polymer systems. 3. Constitutive equation,” *J. Chem. Soc., Faraday Trans. 2* **74**, 1818–1832 (1978).
- Garritano, R., and H. Berting, “Polymer melt and elastomer extension fixture,” US Patent No. 7,096,728 (08/29/2006).
- Hassager, O., J. M. R. Marín, K. Yu, and H. K. Rasmussen, “Polymeric liquids in extension: Fluid mechanics or rheometry?” *Rheol. Acta* **49**, 543–554 (2010).
- Kolte, M. I., H. K. Rasmussen, and O. Hassager, “Transient filament stretching rheometer. 2. Numerical simulation,” *Rheol. Acta* **36**, 285–302 (1997).

- Lyhne, A., H. K. Rasmussen, and O. Hassager, "Simulation of elastic rupture in extension of entangled monodisperse polymer melts," *Phys. Rev. Lett.* **102**, 138301 (2009).
- Marín, J. M. R., and H. K. Rasmussen, "Lagrangian finite-element method for the simulation of K-BKZ fluids with third order accuracy," *J. Non-Newtonian Fluid Mech.* **156**, 177–188 (2009).
- Marrucci, G., and G. Ianniruberto, "Interchain pressure effect in extensional flows of entangled polymer melts," *Macromolecules* **37**, 3934–3942 (2004).
- Meissner, J., and J. Hostettler, "A new elongational rheometer for polymer melts and other highly viscoelastic liquids," *Rheol. Acta* **33**, 1–21 (1994).
- Münstedt, H., "New universal extensional rheometer for polymer melts—Measurements on a polystyrene sample," *J. Rheol.* **23**, 421–436 (1979).
- Nielsen, J. K., and H. K. Rasmussen, "Reversed extension flow," *J. Non-Newtonian Fluid Mech.* **155**, 15–19 (2008).
- Nielsen, J. K., H. K. Rasmussen, and O. Hassager, "Stress relaxation of narrow molar mass distribution polystyrene following uni-axial extension," *J. Rheol.* **52**, 885–899 (2008).
- Rasmussen, H. K., J. H. Christensen, and S. Gøtttsche, "Inflation of polymer melts into elliptic and circular cylinders," *J. Non-Newtonian Fluid Mech.* **93**, 245–263 (2000).
- Rasmussen, H. K., and O. Hassager, "The role of surface tension on the elastic decohesion of polymeric filaments," *J. Rheol.* **45**, 527–537 (2001).
- Rasmussen, H. K., J. K. Nielsen, A. Bach, and O. Hassager, "Viscosity overshoot in the start-up of uniaxial elongation of low density polyethylene melts," *J. Rheol.* **49**, 369–381 (2005).
- Rasmussen, H. K., A. L. Skov, J. K. Nielsen, and P. Laillé, "Elongational dynamics of multiarm polystyrene," *J. Rheol.* **53**, 401–415 (2009).
- Schieber, J. D., D. M. Nair, and T. Kitkrailard, "Comprehensive comparisons with nonlinear flow data of a consistently unconstrained Brownian slip-link model," *J. Rheol.* **51**, 1111–1141 (2007).
- Sentmanat, M. L., "Miniature universal testing platform: From extensional melt rheology to solid-state deformation behaviour," *Rheol. Acta* **43**, 657–669 (2004).
- Sentmanat, M. L., B. N. Wang, and G. H. McKinley, "Measuring the transient extensional rheology of polyethylene melts using the SER universal testing platform," *J. Rheol.* **49**, 585–606 (2005).
- Sizaire, R., and V. Legat, "Element simulation of a filament stretching extensional rheometer," *J. Non-Newtonian Fluid Mech.* **71**, 89–107 (1997).
- Sridhar, T., V. Tiratmadja, D. A. Nguyen, and R. K. Gupta, "Measurement of extensional viscosity of polymer-solutions," *J. Non-Newtonian Fluid Mech.* **40**, 271–280 (1991).
- Szabo, P., "Transient filament stretching rheometer. I. Force balance analysis," *Rheol. Acta* **36**, 277–284 (1997).
- Wagner, M. H., S. Kheirandish, and O. Hassager, "Quantitative prediction of transient and steady-state elongational viscosity of nearly monodisperse polystyrene melts," *J. Rheol.* **49**, 1317–1327 (2005).
- Wagner, M. H., and V. H. Rolón-Garrido, "The interchain pressure effect in shear rheology," *Rheol. Acta* **49**, 459–471 (2010).
- Wagner, M. H., V. H. Rolón-Garrido, J. K. Nielsen, H. K. Rasmussen, and O. Hassager, "A constitutive analysis of transient and steady-state elongational viscosities of bidisperse polystyrene blends," *J. Rheol.* **52**, 67–86 (2008).
- Wagner, M. H., and J. Schaeffer, "Nonlinear strain measures for general biaxial extension of polymer melts," *J. Rheol.* **36**, 1–26 (1992).
- Wang, Y., P. Boukany, S.-Q. Wang, and X. Wang, "Elastic breakup in uniaxial extension of entangled polymer melts," *Phys. Rev. Lett.* **99**, 237801 (2007).
- Wang, Y., and S.-Q. Wang, "From elastic deformation to terminal flow of a monodisperse entangled melt in uniaxial extension," *J. Rheol.* **52**, 1275–1290 (2008).
- Webster, M. F., H. Matallah, K. S. Sujatha, and M. J. Banaai, "Numerical modelling of step-strain for stretched filaments," *J. Non-Newtonian Fluid Mech.* **151**, 38–58 (2008).
- Yu, K., J. M. R. Marín, H. K. Rasmussen, and O. Hassager, "3D modeling of dual wind-up extensional rheometers," *J. Non-Newtonian Fluid Mech.* **165**, 14–23 (2010).